Cell Reports, Volume *22*

Supplemental Information

Oxygen-Sensitive Remodeling of Central Carbon Metabolism by Archaic eIF5B

J.J. David Ho, Nathan C. Balukoff, Grissel Cervantes, Petrice D. Malcolm, Jonathan R. Krieger, and Stephen Lee

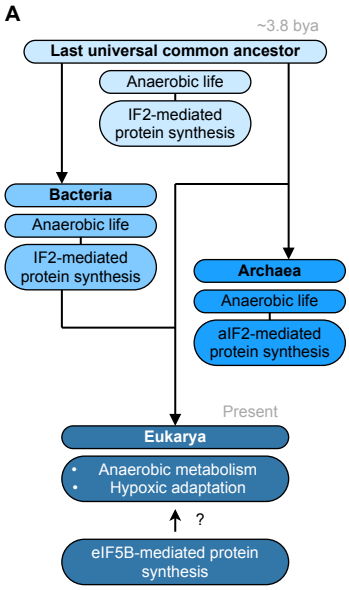

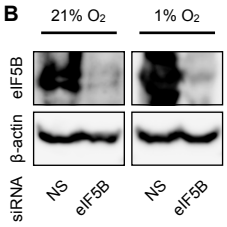

C **Relative areas under the curve for eIF5B knockdown ribosome density profiles**

21% O_2 - Area	Monosome	Oligosome	Polysome
NS siRNA	1.00	1.00	1.00
eIF5B siRNA	1.23	0.91	0.86
		Average = 0.88	

1% O_2 - Area	Monosome	Oligosome	Polysome
NS siRNA	1.00	1.00	1.00
eIF5B siRNA	1.10	**0.85**	**0.48**
		Average = **0.66**	

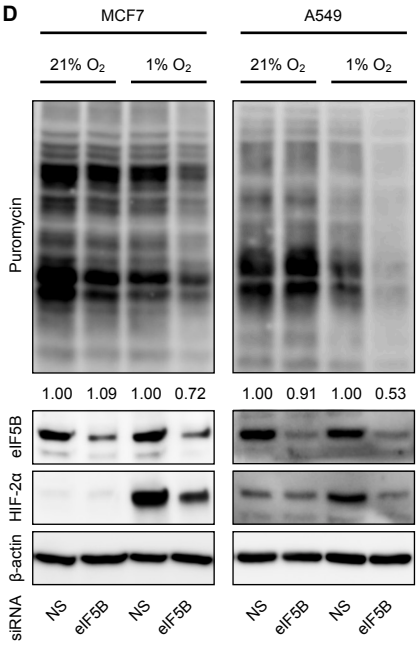

Figure S1. Related to Figure 1. (A) Model for the hypothesis that eIF5B was conserved throughout the evolution of aerobic eukaryotes for hypoxic adaptation and metabolism. IF2/eIF5B likely evolved in the last universal common ancestor under anaerobic conditions, and contemporary bacterial and archaeal IF2 homologs are capable of performing protein synthesis during oxygen deficiency. **(B)** Validation of siRNA-mediated eIF5B knockdown success by immunoblot for Figure 1D. Representative immunoblots are shown. **(C)** Area under curve measurements of ribosome density profiles of normoxic and hypoxic U87MG treated with control non-silencing (NS) or eIF5B-specific siRNA (Figure 1D). **(D)** Representative immunoblots of normoxic and hypoxic MCF7 and A549 treated with NS or eIF5B-specific siRNA.

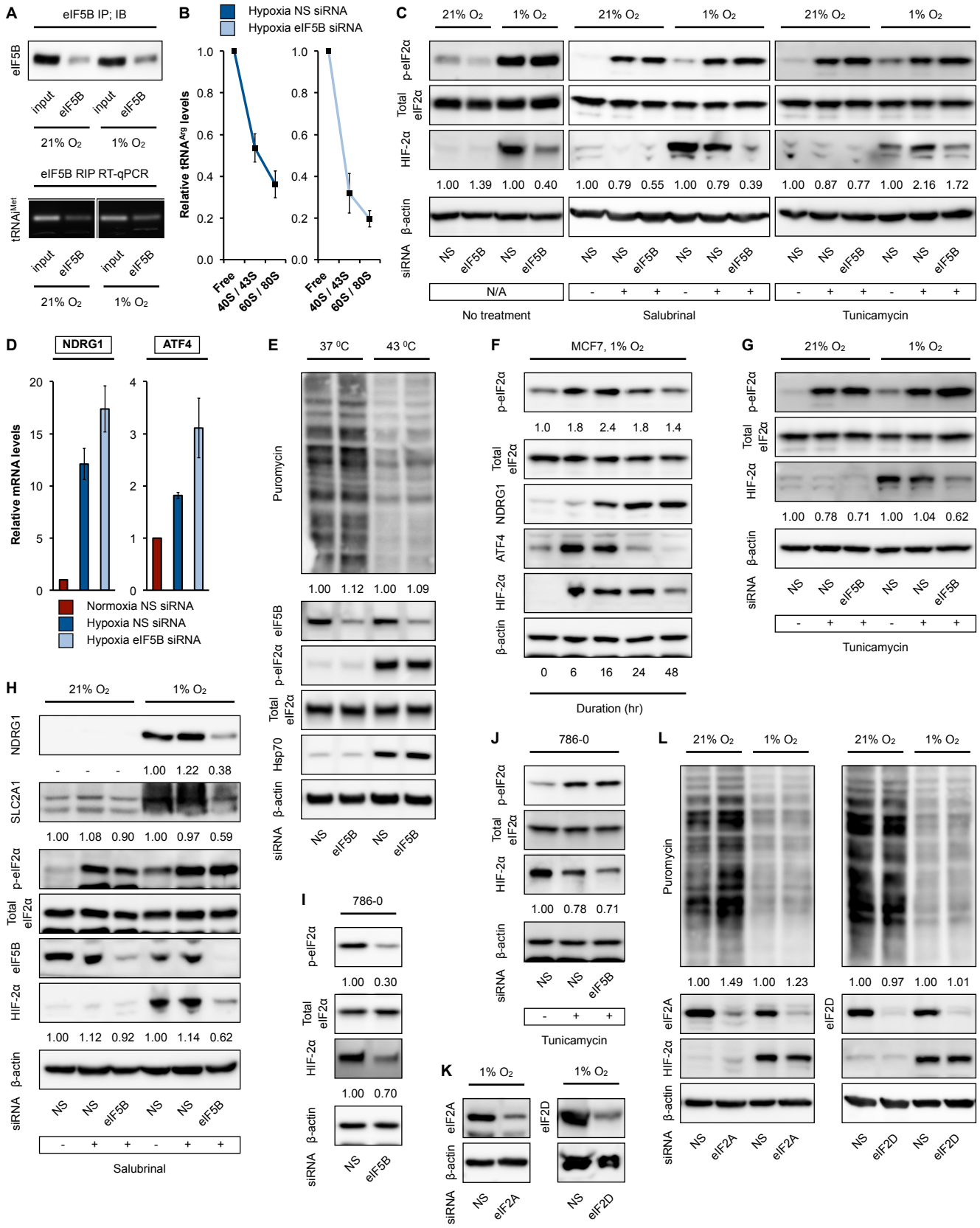
A
eIF5B IP; IB
eIF5B
input
eIF5B
input
eIF5B
21% O2
1% O2
eIF5B RIP RT-qPCR
tRNAiMet
input
eIF5B
input
eIF5B
21% O2
1% O2
B
Hypoxia NS siRNA
Hypoxia eIF5B siRNA
Relative tRNAArg levels
Free
40S / 43S
60S / 80S
Free
40S / 43S
60S / 80S
C
21% O2
1% O2
21% O2
1% O2
21% O2
1% O2
p-eIF2α
Total eIF2α
HIF-2α
1.00 1.39 1.00 0.40 1.00 0.79 0.55 1.00 0.79 0.39 1.00 0.87 0.77 1.00 2.16 1.72
β-actin
siRNA
NS
eIF5B
NS
eIF5B
NS
NS
eIF5B
NS
NS
eIF5B
NS
NS
eIF5B
NS
NS
eIF5B
N/A
- + + - + +
- + + - + +
No treatment
Salubrinal
Tunicamycin
D
NDRG1
ATF4
Relative mRNA levels
Normoxia NS siRNA
Hypoxia NS siRNA
Hypoxia eIF5B siRNA
E
37 °C
43 °C
Puromycin
1.00 1.12 1.00 1.09
eIF5B
p-eIF2α
Total eIF2α
Hsp70
β-actin
siRNA
NS
eIF5B
NS
eIF5B
F
MCF7, 1% O2
p-eIF2α
1.0 1.8 2.4 1.8 1.4
Total eIF2α
NDRG1
ATF4
HIF-2α
β-actin
0 6 16 24 48
Duration (hr)
G
21% O2
1% O2
p-eIF2α
Total eIF2α
HIF-2α
1.00 0.78 0.71 1.00 1.04 0.62
β-actin
siRNA
NS
NS
eIF5B
NS
NS
eIF5B
- + + - + +
Tunicamycin
H
21% O2
1% O2
NDRG1
- - - 1.00 1.22 0.38
SLC2A1
1.00 1.08 0.90 1.00 0.97 0.59
p-eIF2α
Total eIF2α
eIF5B
HIF-2α
1.00 1.12 0.92 1.00 1.14 0.62
β-actin
siRNA
NS
NS
eIF5B
NS
NS
eIF5B
- + + - + +
Salubrinal
I
786-0
p-eIF2α
1.00 0.30
Total eIF2α
HIF-2α
1.00 0.70
β-actin
siRNA
NS
eIF5B
J
786-0
p-eIF2α
Total eIF2α
HIF-2α
1.00 0.78 0.71
β-actin
siRNA
NS
NS
eIF5B
- + +
Tunicamycin
K
1% O2
1% O2
eIF2A
eIF2D
β-actin
siRNA
NS
eIF2A
NS
eIF2D
L
21% O2
1% O2
21% O2
1% O2
Puromycin
1.00 1.49 1.00 1.23
1.00 0.97 1.00 1.01
eIF2A
eIF2D
HIF-2α
β-actin
siRNA
NS
eIF2A
NS
eIF2A
NS
eIF2D
NS
eIF2D

Figure S2. Related to Figure 2. (A) Validation of eIF5B IP by immunoblot (top panel) and agarose gel images of RT-qPCR products after 40 amplification cycles (bottom panel) for Figure 2A. Representative images are shown. **(B)** Normoxic and hypoxic U87MG treated with control non-silencing (NS) or eIF5B-specific siRNA were subjected to ribosome density fractionation, followed by RT-qPCR measurements of elongator $tRNA^{Arg}$ levels in free, 40S/43S, and 60S/80S fractions. **(C)** Representative control immunoblots for Figure 2D. **(D)** Normoxic and hypoxic U87MG treated with control non-silencing (NS) or eIF5B-specific siRNA were subjected to ribosome density fractionation, followed by RT-qPCR measurements of NDRG1 and ATF4 steady-state mRNA levels (based on aggregate abundance across all fractions). **(E)** Representative immunoblots of U87MG exposed to 4 hr of heat shock (43 ^{0}C) versus untreated controls (37 ^{0}C). **(F)** Representative immunoblots of hypoxic (time course) MCF7. **(G)** Representative control immunoblots for Figure 2G. **(H)** Representative immunoblots of normoxic and hypoxic (24 hr) U87MG treated with NS or eIF5B-specific siRNA and salubrinal. **(I)** Representative control immunoblots for Figure 2H. **(J)** Representative control immunoblots for Figure 2J. **(K)** Validation of siRNA-mediated eIF2A and eIF2D knockdown success by immunoblot for Figure 2K. Representative immunoblots are shown. **(L)** Representative immunoblots of normoxic and hypoxic U87MG treated with NS, eIF2A-specific (left panel), or eIF2D-specific (right panel) siRNA.

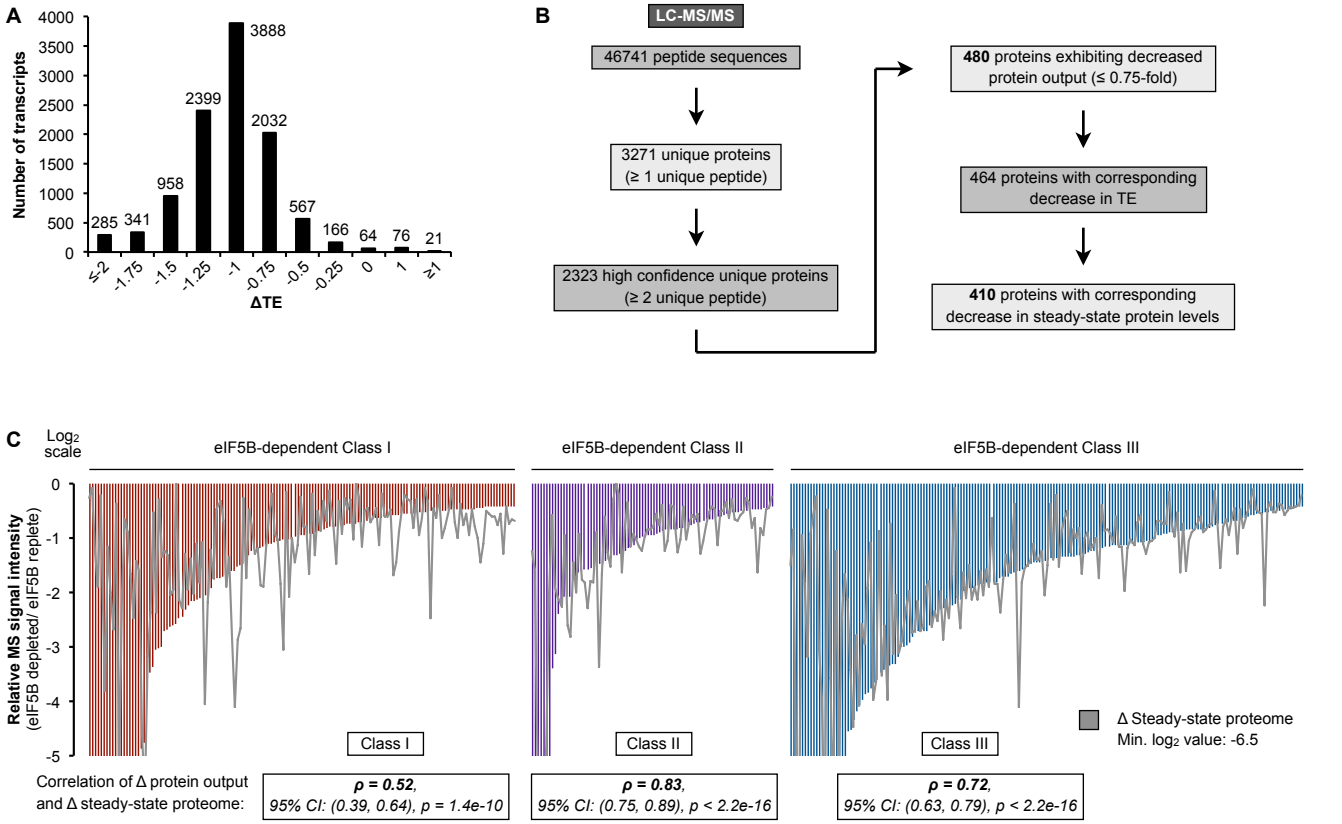

Figure S3. Related to Figure 3. (A) Transcript distribution profile of TE changes in eIF5B depleted (eIF5B-specific siRNA) versus eIF5B replete (control non-silencing (NS) siRNA), hypoxic U87MG cells. **(B)** Liquid chromatography tandem mass spectrometry (LC-MS/MS) analysis workflow for identifying eIF5B-dependent targets that show concordant changes in TE, protein output, and steady-state protein level. **(C)** Correlation between protein output and steady-state protein level for eIF5B-dependent targets classified based on hypoxia-responsiveness. Class I and III members are preferentially translated in normoxia and hypoxia, respectively, whereas Class II members are translated across oxygen levels.

A **KEGG pathway enrichment analysis of eIF5B-dependent targets**

KEGG pathway	*KEGG identifier term(s)*	*Lowest p value*	*Benjamini-corrected p value*	*Fold enrichment*
Carbon metabolism	hsa01200	1.80e-07	2.21e-05	4.20
Glycolysis	hsa00010	4.30e-04	8.11e-03	3.90
TCA cycle	hsa00020	1.89e-04	7.71e-03	6.33
Pentose phosphate pathway	hsa00030	6.52e-03	5.78e-02	4.91
Pyruvate metabolism	hsa00620	5.97e-03	5.51e-02	4.16
Oxidative phosphorylation	hsa00190	9.76e-03	7.27e-02	2.32
Hypoxic adaptation	hsa04066, hsa04151, hsa04370	2.55e-03	3.42e-03	2.91
Amino acid synthesis and protein processing	hsa01230, hsa04141	2.32e-04	6.32e-03	3.85
Cell adhesion	hsa04015, hsa04510, hsa04512, hsa04540	3.06e-06	2.51e-04	4.32
Endocytosis	hsa04144, hsa04145	1.91e-04	6.70e-03	2.30

B

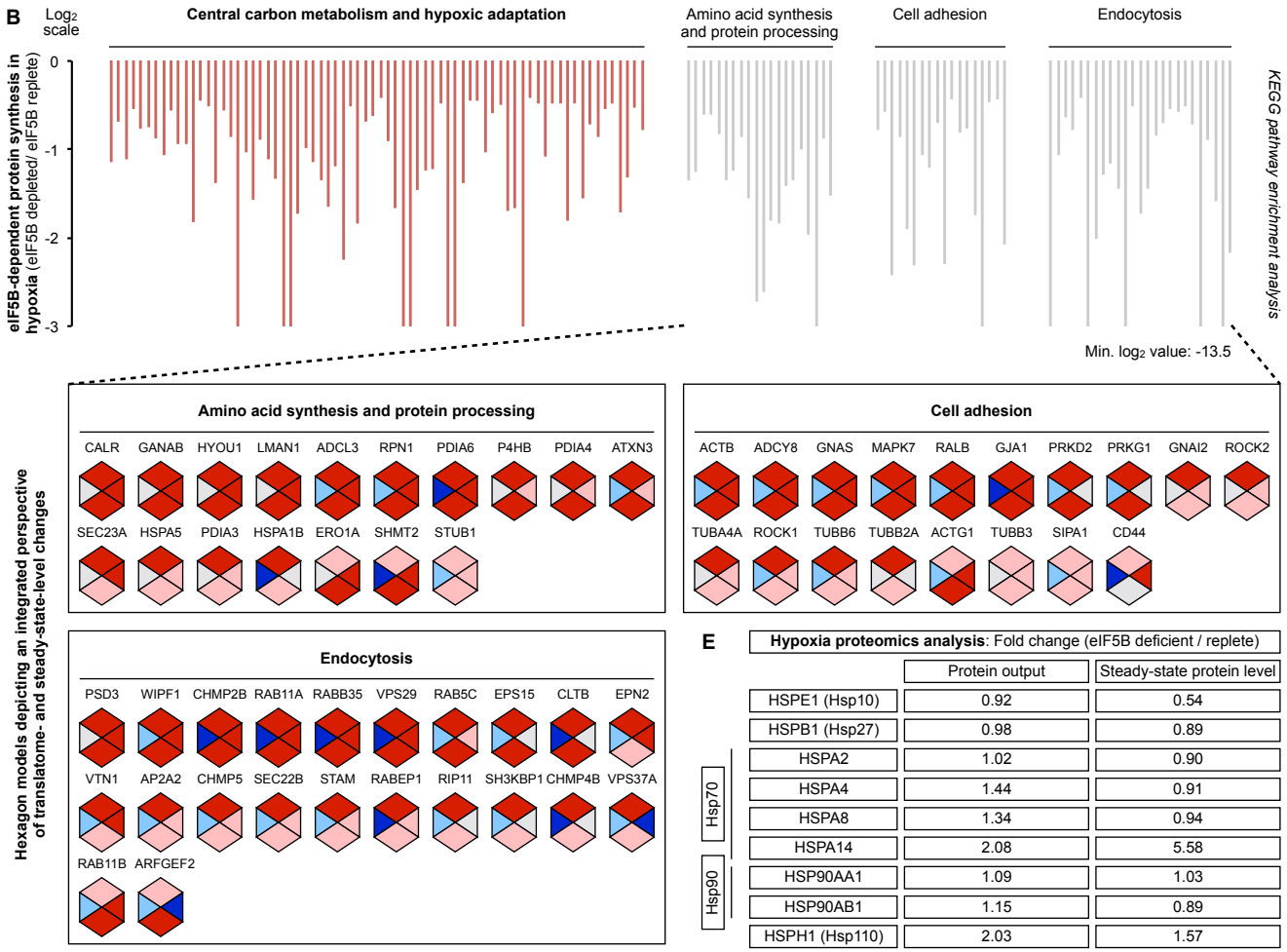

C

	Class I	Class II	**Class III**
Central carbon metabolism and hypoxic adaptation	15 (21%)	10 (14%)	47 (**65%**)
Amino acid synthesis and protein processing	4 (20%)	2 (10%)	14 (**70%**)
Cell adhesion	5 (27.7%)	3 (16.7%)	10 (**55.6%**)
Endocytosis	11 (44%)	4 (16%)	10 (**40%**)

D

* Reaction	Enzymes
Fructose 6-P ⇄ Fructose 1,6-BP	PFKP, PFKL, PFKM, PFKFB3, PFKFB4
2-Phosphoglycerate ⇄ PEP	ENO2, ENO1, ENO3
Pyruvate → Acetyl CoA	PDHA1, PDHB, PDHX, DLD
Succinate ⇄ Fumarate	SDHA, SDHAF1, SDHAF2, SDHAF4, SDHAP1

Legend: eIF5B-dependent; identified by TE analysis — eIF5B-dependent; identified by TE and protein output analyses

E **Hypoxia proteomics analysis**: Fold change (eIF5B deficient / replete)

		Protein output	Steady-state protein level
Hsp70	HSPE1 (Hsp10)	0.92	0.54
	HSPB1 (Hsp27)	0.98	0.89
	HSPA2	1.02	0.90
	HSPA4	1.44	0.91
	HSPA8	1.34	0.94
	HSPA14	2.08	5.58
Hsp90	HSP90AA1	1.09	1.03
	HSP90AB1	1.15	0.89
	HSPH1 (Hsp110)	2.03	1.57

F

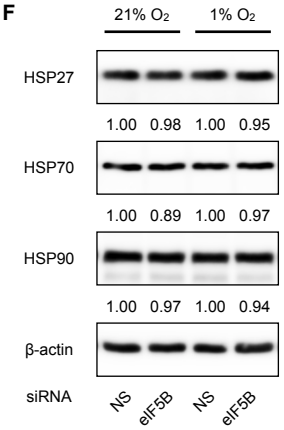

G

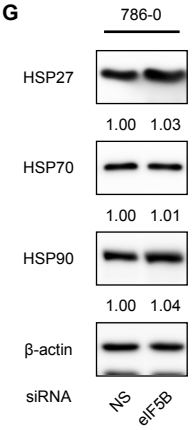

Figure S4. Related to Figure 4. (**A, B,** top panel) KEGG pathway enrichment analysis of eIF5B-dependent cellular systems. (**B,** bottom panel) Hexagon models are shown, depicting TE, steady-state RNA level, protein output, and steady-state protein level for each individual detected protein involved in amino acid synthesis and protein processing, cell adhesion, and endocytosis. Legend is shown in Figure 4B. **(C)** Distribution of eIF5B-dependent targets across the three hypoxia-responsive classes. **(D)** Full list of eIF5B-dependent enzymes and/or isoforms identified to participate in the specific central carbon metabolism pathways. **(E)** Change in protein output and steady-state protein levels for heat shock proteins in eIF5B depleted (eIF5B-specific siRNA) versus eIF5B replete (control non-silencing (NS) siRNA), hypoxic U87MG cells. Representative immunoblots of **(F)** normoxic and hypoxic U87MG cells and **(G)** normoxic 786-0 treated with NS or eIF5B-specific siRNAs.

Supplemental Experimental Procedures. Related to Experimental Procedures.

Mass spectrometry analysis. Samples were re-suspended in 100 uL of 50 mM NH_4HCO_3 (pH 8.3), 8 M Urea, and DTT was added to reduce cysteines at a final concentration of 10 mM. Cysteines were reduced at 60°C for 1 hour. Sample was cooled to room temperature and iodoacetamide was added to a final volume of 20 mM. Samples were incubated at room temperature in the dark for 30 min. Samples were then acetone precipitated overnight, and protein precipitates were centrifuged at 23,000 g for 15 min. Precipitates were re-suspended in 50 uL of NH_4HCO_3 (pH 8.3), and MS grade Trypsin/LysC (Promega) was added to a final protease:protein ratio of 1:50 and samples were digested overnight at 37 ^{0}C. Samples were lyophilized and re-suspended in 0.1% trifluoroacetic acid (TFA). Peptides were fractionated using the Pierce High pH Reverse Phase Peptide Fractionation Kit (Pierce), following the manufacturer's instructions. Each sample was fractionated into 8 high pH fractions.

Fractionated peptides were lyophilized, and lyophilized peptide mixtures were dissolved in 0.1% formic acid and loaded onto a 75 μm x 2 cm PepMap 100 Easy-Spray pre-column filled with 3 μm C18 beads (Thermo Fisher Scientific) followed by an in-line 75 μm x 50 cm PepMap RSLC EASY-Spray column filled with 2 μm C18 beads (Thermo Fisher Scientific) at a pressure of 700 BAR. Peptides were eluted over 120 to 240 min at a rate of 250 nl/min using a 0 to 35% acetonitrile gradient in 0.1 % formic acid. For ribosome density fractionated samples, "free" fractions were eluted over 120 min each, while "40/60/80S" and "polysome" fractions were eluted over 180 each. eIF5B-depleted and control samples were eluted over 240 min each. Peptides were introduced by nanoelectrospray into an LTQ-Orbitrap Elite hybrid mass spectrometer (Thermo-Fisher) outfitted with a nanospray source and EASY-nLC split-free nano-LC system (Thermo Fisher Scientific). The instrument method consisted of one MS full scan (400–1500 m/z) in the Orbitrap mass analyzer, an automatic gain control target of 1e6 with a maximum ion injection of 200 ms, one microscan, and a resolution of 240,000. Ten data-dependent MS/MS scans were performed in the linear ion trap using the ten most intense ions at a normalized collision energy of 35. The MS and MS/MS scans were obtained in parallel fashion. In MS/MS mode automatic gain control targets were 1e5 with a maximum ion injection time of 50 ms. A minimum ion intensity of 5000 was required to trigger an MS/MS spectrum. Dynamic exclusion was applied using a maximum exclusion list of 500 with one repeat count with a repeat duration of 30 s and exclusion duration of 15 s.

Raw MS files acquired from the mass spectrometer were processed using PEAKS software (Bioinformatics Solutions Inc.). Data was loaded into the software program and data from each fraction was refined to merge scans within 2 min and 10.0 ppm. Spectra with PEAKS filter scores <0.5 were excluded. *De novo* sequencing and database searching was done using a precursor mass cutoff of 10.0 ppm and a fragment mass tolerance of 0.6 Da. Carbidomethylation of cysteine (+57.02 Da) residues was selected as a fixed modification while variable modifications included $^{13}C_6$-$^{15}N_2$ SILAC on K (8.01Da), $^{13}C_6$-$^{15}N_4$ SILAC on R (10.02), Oxidation of M (15.99). Label-free quantification was performed in PEAKS using SILAC labels. Data sets are available at the PRoteomics IDEntifications (PRIDE) database via ProteomeXchange, accession PXD006799.

RNA interference. Small interfering RNA (siRNA) pools (siGENOME siRNA, GE Dharmacon) were transfected at a final concentration of 50 nM using Effectene (Qiagen) for 48 hr.

Cell viability assays. Fluorescein diacetate (FDA) staining was used to assess cell viability. Briefly, cells were incubated in FDA (10 μg/ml) for 30 min at 37^0C with DAPI counterstaining, and visualized with fluorescence microscopy (excitation and emission wavelengths of 492 nm and 517 nm, respectively) after washing with PBS. In addition, cell viability measurements were performed using the RealTime-Glo MT Cell Viability Assay (Promega) at indicated time points over 48 hr on cells grown in the same well.

Global protein synthesis measurements. Global protein synthesis was measured by puromycin (Thermo Fisher Scientific) incorporation (1 μg/ml) for 20 min, followed by immunoblot analysis with an anti-puromycin antibody (see below).

Immunoblot. Immunoblots were performed using standard techniques using the following antibodies: β-actin (Thermo Fisher Scientific, MA5-15739), ATF4 (Cell Signaling Technology, 11815S), total eIF2α (Cell Signaling Technology, 5324), Ser51-phosphorylated eIF2α (Abcam, ab32157), eIF2A (Proteintech, 11233-1-AP), eIF2D (Proteintech, 12840-1-AP), eIF5B (Santa Cruz Biotechnology, sc-393564), GLUT1 (Novus Biologicals, NB110-39113), HIF-2α (Novus Biologicals, NB100-122), HSP27 (Cell Signaling Technology, 2402S), HSP70 (Santa Cruz Biotechnology, sc-66048), HSP90 (Cell Signaling Technology, 4877S), NDRG1 (Abcam, ab37897), P4HA1 (Novus

Biologicals, NB100-57852), and puromycin (EMD Millipore, MABE343). HRP-conjugated secondary antibodies (Santa Cruz Biotechnology) were used. Signals were detected by chemiluminescence (Pierce) using an Amersham Imager 600 (GE Healthcare Life Sciences) and analyzed in ImageJ (NIH).

RNA immunoprecipitation. eIF5B RNA immunoprecipitation (RIP) experiments were performed using the Imprint RNA Immunoprecipitation Kit (Sigma-Aldrich) according to the manufacturer's protocols. Whole cell lysates extracted with mild lysis buffer were incubated with an eIF5B/IF2-specific antibody (Bethyl Laboratories Inc., A301-744A) at 4 ^{0}C overnight. 200 µl of lysate and 7.5 µg of pre-bound antibodies were used for each RIP reaction.

Reverse transcription-quantitative polymerase chain reaction (RT-qPCR). First-strand cDNA synthesis was performed using the High-Capacity cDNA Reverse Transcription Kit (Thermo Fisher Scientific), according to the manufacturer's protocol. qRT-PCR was performed using the PowerUp SYBR Green Master Mix (Thermo Fisher Scientific) and a StepOnePlus Real-Time PCR System (Applied Biosystems, Thermo Fisher Scientific). All primer sequences are available upon request. Relative changes in expression were calculated using the comparative Ct ($\Delta\Delta$Ct) method.

RNA-sequencing and analysis. Equal volumes of relevant ribosome density fractionated fractions were combined to yield the "free", "40/60/80S", and "polysome" samples, respectively. Poly(A) RNA selection, library preparation, and RNA sequencing were performed by the Sylvester Comprehensive Cancer Center Oncogenomics Core Facility, using the KAPA Stranded mRNA-Seq Kit (KAPA Biosystems) and NextSeq 500 High Output Kit v2 (Illumina). Paired-end (2 x 75 bp) sequencing runs at a depth of >50 million reads were performed on the libraries using the NextSeq 500 system (Illumina).

Raw data pre-processing was performed by the Sylvester Comprehensive Cancer Center Biostatistics and Bioinformatics Core Facility. For differential expression analysis, raw paired-end read data in FASTQ format were assessed for quality with FastQC (v. 11.5, Babraham Bioinformatics). Trimmomatic (Bolger et al., 2014) (v. 0.32) was used to remove adapters, Illumina-platform specific sequences, and low quality leading and trailing bases.

STAR (Dobin et al., 2013) ((v. 2.5.0) was then utilized to map reads to the reference transcriptome (UCSC hg38 knownGene database). Results were then processed by SAMtools (Li et al., 2009) (v. 0.1.19) for assignment to genomic features using featureCounts (Liao et al., 2014) in the Subread package (Liao et al., 2013) (v. 1.5.0). Transcript quantification (Fragments Per Kilobase of transcript per Million mapped reads, FPKM) was performed with RSEM (Li and Dewey, 2011) (v. 1.2.31) with a reference transcriptome (gencode.v26.p10.h38). Following input adjustment, translation efficiency was calculated based on polysomal to monosomal FPKM ratio. Steady-state RNA (transcriptome) levels were calculated based on the sum of FPKM across all fractions. Data sets are available at the NCBI Sequence Read Archive (SRA) database, accession SRP110475.

Kyoto Encyclopedia of Genes and Genomes (KEGG) pathway enrichment analysis. KEGG analysis was performed using the Database for Annotation, Visualization, and Integrated Discovery (DAVID) bioinformatics resource (Huang da et al., 2009) (v. 6.8).

Supplemental References

Bolger, A.M., Lohse, M., and Usadel, B. (2014). Trimmomatic: a flexible trimmer for Illumina sequence data. Bioinformatics *30*, 2114-2120.

Dobin, A., Davis, C.A., Schlesinger, F., Drenkow, J., Zaleski, C., Jha, S., Batut, P., Chaisson, M., and Gingeras, T.R. (2013). STAR: ultrafast universal RNA-seq aligner. Bioinformatics *29*, 15-21.

Huang da, W., Sherman, B.T., and Lempicki, R.A. (2009). Systematic and integrative analysis of large gene lists using DAVID bioinformatics resources. Nat Protoc *4*, 44-57.

Li, B., and Dewey, C.N. (2011). RSEM: accurate transcript quantification from RNA-Seq data with or without a reference genome. BMC Bioinformatics *12*, 323.

Li, H., Handsaker, B., Wysoker, A., Fennell, T., Ruan, J., Homer, N., Marth, G., Abecasis, G., Durbin, R., and Genome Project Data Processing, S. (2009). The Sequence Alignment/Map format and SAMtools. Bioinformatics *25*, 2078-2079.

Liao, Y., Smyth, G.K., and Shi, W. (2013). The Subread aligner: fast, accurate and scalable read mapping by seed-and-vote. Nucleic Acids Res *41*, e108.

Liao, Y., Smyth, G.K., and Shi, W. (2014). featureCounts: an efficient general purpose program for assigning sequence reads to genomic features. Bioinformatics *30*, 923-930.